JCTC Journal of Chemical Theory and Computation

Low Inhibiting Power of N···CO Based Peptidomimetic Compounds against HIV-1 Protease: Insights from a QM/MM Study

Julian Garrec,[†,||] Michele Cascella,[‡] Ursula Rothlisberger,[§] and Paul Fleurat-Lessard*[,†]

Université de Lyon, École Normale Supérieure de Lyon, Laboratoire de Chimie − UMR 5182, 46 allée d'Italie, 69364 Lyon Cedex 07, France, Department of Chemistry and Biochemistry, University of Bern, Freiestrasse 3, CH-3012 Bern, Switzerland, and Laboratory of Computational Chemistry and Biochemistry, Institute of Chemical Sciences and Engineering, École Polytechnique Fédérale de Lausanne, CH-1015 Lausanne, Switzerland

Received September 8, 2009

Abstract: Recently, Hasserodt et al. proposed new HIV-1 drug candidates based on a weak N···CO interaction, designed to be a close transition state analog (Gautier et al. *Bioorg. Med. Chem.* **2006**, *14*, 3835−3847; Waibel et al. *J. Bioorg. Med. Chem.* **2009**, *17*, 3671−3679). They suggested that further improvement of these compounds could take advantage of computational approaches. In the present work, we propose an atomistic model based on a QM/MM description of the N···CO core embedded in an amino-aldehyde peptidic inhibitor. We focus on the existence of the N···CO interaction in the aqueous and enzymatic media. We show that the N···CO bond holds in water, while in the protein, there is a competition between the formation of the weak N···CO bond and the conservation of the hydrogen bond network around the structural water molecule W301 that is known to be crucial for the binding of both substrates and inhibitors. This competition hampers the inhibitor to provide strong stabilizing interactions with all the key parts of the protein at the same time. Our calculations indicate that this competition we observed in peptidic compounds might be avoided by the proper design of nonpeptidic ones, following a similar strategy to that for cyclic urea derivatives and the FDA approved drug Tipranavir. Hence, our results encourage further development of the nonpeptidic hydrazino-urea derivatives suggested recently by Hasserodt et al.

1. Introduction

The human immunodeficiency virus type 1 aspartic protease (HIV-1 PR, Figure 1) is one of the major targets for the design of anti-AIDS drugs.[1,2] This enzyme catalyzes the hydrolysis at specific sites of the polyprotein encoded by the virus genome yielding separate functional proteins.[3−5] This function was shown early to be crucial to virion assembly and maturation, and its disruption by either active-site mutation or inhibition leads to the production of viral particles that lack infectious ability.[6−8]

Several HIV-1 PR inhibitors have been approved by the FDA and significantly prolong the life expectancy of HIV infected patients.[1,9−11] Nevertheless, the rapid emergence of resistance caused by multiple HIV-1 PR mutations decreases the effectiveness of these drugs.[9,12,13] Almost all FDA-approved drugs are peptidomimetic active-site inhibitors that contain a hydroxyl group designed to interact with the central

* To whom correspondence should be addressed. Phone: +33 4 7272 8154, Fax: +33 4 7272 8860. E-mail: Paul.Fleurat-Lessard@ens-lyon.fr.

[†] École Normale Supérieure de Lyon.

[‡] University of Bern.

[§] École Polytechnique Fédérale de Lausanne.

[||] Present address: Laboratory of Computational Chemistry and Biochemistry, Institute of Chemical Sciences and Engineering, École Polytechnique Fédérale de Lausanne, CH-1015 Lausanne, Switzerland.

10.1021/ct9004728
Published on Web 03/26/2010

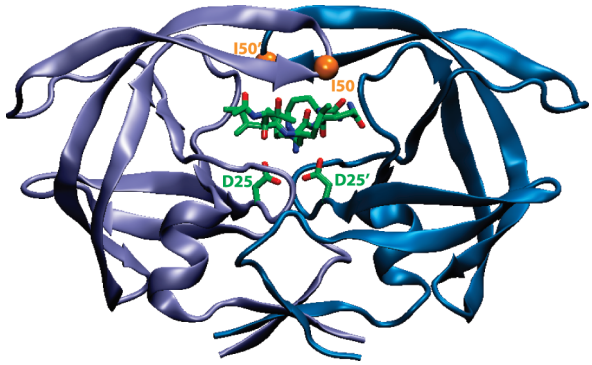

Figure 1. Crystallographic structure of HIV-1 PR in complex with the peptidomimetic inhibitor MVT-101[36,34] (4HVP entry in the PDB data bank[44]). The *aspartyl dyad* (residues 25 and 25′) is located in the lower part of the active site. Ile 50 and 50′ are located at the flap tips and are indicated with orange spheres. Drawings were made with the VMD program.[83]

aspartyl dyad of HIV-1 PR (see the Abbreviations section for a list of abbreviations used in this work).[1,2]

Freire et al. suggested that the competitive advantage of HIV-1 PR inhibitors over substrate binding is probably due to their higher rigidity, providing a more favorable entropic change upon binding. However, because of their rigidity, these inhibitors are less amenable to adapt to shape modifications of the enzymatic binding site induced by mutations.[14] Hence, the design of new potent inhibitors that exhibit both a better binding free energy and an increased flexibility remains a challenging task.[13,15−17]

In that context, finding functional groups that yield stronger interactions with the aspartyl dyad than the usual hydroxyl group would be of great interest.[18] Toward this aim, Hasserodt et al.[19−21] proposed a new concept of aspartic protease inhibitors based on a noncovalent interaction of a tertiary amine nitrogen with a carbonyl group, the so-called N···CO bond, that they believed to be a better transition state analog than the commonly used hydroxyl moiety (Figure 2). As a first attempt, they synthesized a series of dipeptide mimics containing the N···CO core,[19] the amine and aldehyde fragments being bridged by an ethylene moiety (referred to as the *aliphatic bridge* hereafter, Figure 2a).

The best candidate of these amino-aldehyde peptides (AAP) exhibited an inhibition constant of 97 μM, far from the typical picomolar value that is desirable for a potent inhibitor.[15,17,22−25]

In order to design more efficient inhibitors, they synthesized new compounds based on hydrazyno-urea heterocycles containing both the N···CO core and a carbonyl group aimed at forming hydrogen bonds with two NH groups of the upper part of the HIV-1 PR active site,[20,21] the so-called *flaps*. This strategy is similar to that involved in the design of cyclic urea derivatives[26] and the FDA-approved drug Tipranavir.[27] The hydrazyno-urea derivatives indeed proved to interact slightly stronger with HIV-1 PR ($K_i \approx 29$ μM for the best candidate). Hasserodt et al. concluded that a hit to lead optimization could now be initiated with the help of computational methods.[20,21] Such an approach, however, needs the definition of a proper model describing the N···CO core in a biological environment. The purpose of the present work is to design this model and to apply it to AAPs in order to help elucidate the origin of their low inhibition power.

Using a mixed quantum mechanics/molecular mechanics (QM/MM)[28] approach, we have designed a model that explicitly includes the solvated enzyme complexed with an AAP. An accurate quantum level of theory is crucial to the correct description of the N···CO core interacting with the aspartyl dyad, due to the intrinsic complexity of this system. No accurate transferable force field parameters exist for the N···CO bond,[29,30] in particular because the stability of the N···CO is highly sensitive to the nature of the surrounding medium.[19,31−33] For instance, the N···CO bond is unstable in apolar-aprotic media, leaving the tertiary amine and the aldehyde groups essentially independent. The structure of a complex between HIV-1 PR and an AAP has not been reported yet. Our study aims at exploring the feasibility of N···CO bond formation in this enzyme. In order to compare the behavior of the AAP, in particular the N···CO bond, in the protein and in aqueous media, we have also designed a similar QM/MM model of the AAP in water.

This article is organized as follows: in the first part, we detail our structural model and the computational procedure used to model the AAP in the enzymatic and aqueous media. Results are reported and discussed in the second part, while the last part summarizes our main findings.

2. Materials and Methods

2.1. Initial Structure. No experimental structure of an AAP complexed with HIV-1 PR (E•AAP) is available. Nonetheless, on the basis of known structural features of HIV-1 PR−substrate complexes and previous kinetics/inhibition experiments of Hasserodt et al., it is possible to construct a starting structure for molecular dynamics simulations. Indeed, inhibition profiles show a competitive mechanism strongly suggesting that the AAP truly binds to the active site of the enzyme.[19] In addition, HIV-1 PR is known to bind a variety of peptide substrates in the same extended conformation,[34,35] the substrate backbone exhibiting many hydrogen bonds with the enzyme and the side chains being accommodated in a series of binding site subpockets. Due to the very high peptidic character of AAPs, their backbone and side chains should bind the active site in a way very similar to that of the corresponding peptides. Since AAPs are designed to be transition state analogs,[19] the reaction intermediate (E•INT) that connects the two TSs along the reaction pathway of HIV-1 PR appears as a natural starting structure for E•AAP modeling.

From both ^{18}O isotope exchange experiments[36] and X-ray structures that captured key intermediate stages of the catalytic reaction,[37,38] there is evidence that the substrate peptide bond cleavage involves the nucleophilic attack of a water molecule onto the scissile peptide bond, leading to a tetrahedral intermediate (Figure 2c). Note that, despite this commonly accepted picture, the protonation state of the intermediate is still a matter of controversy. Indeed, while ab initio calculations suggested that the intermediate is a neutral gem-diol,[39,40] an empirical valence bond (EVB) model—calibrated against DFT calculations involving model

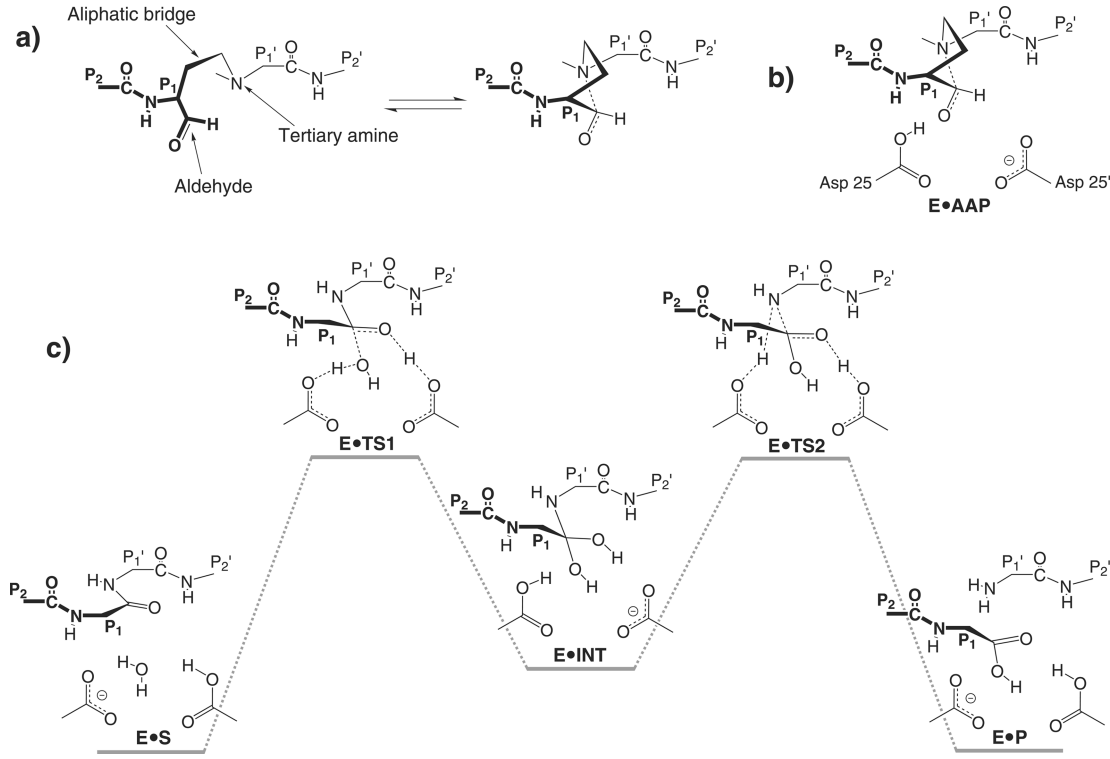

Figure 2. N···CO bond as a transition state mimic. (a) N···CO bond formation within an amino-aldehyde peptide (AAP). Side chains of the AAP are not represented for the sake of simplicity. Instead, their positions are indicated using the notation of Schechter and Berger (P_2, P_1, P'_1, P'_2).[84] The N···CO core is introduced at the $P_1-P'_1$ junction, the proximity of the amine and aldehyde fragments being ensured by an *aliphatic bridge*. (b) HIV-1 PR aspartyl dyad complexed with an AAP. (c) Catalytic mechanism of HIV-1 PR involving a tetrahedral intermediate (E•INT), which is represented here as a gem-diol. Note that some authors have reported that this intermediate could be an oxyanion (see text).[41,42]

compounds in the gas phase—provided evidence for a charged oxyanion.[41] Other authors calibrated their EVB Hamiltonian without including the gem-diol in their resonance structure set.[42] Since we have chosen a computational setup involving an *ab initio* approach similar to that of ref 39, we have considered a neutral gem-diol in the present study. However, we stress that this choice should not affect our results dramatically, since the tetrahedral intermediate is just chosen as a starting structure to perform a first equilibration of the system. More specifically, we chose the complex between HIV-1 PR (E) and the Thr−Ile−Met−Met−Gln−Arg peptide substrate[43] in its hydrated form (INT; Figure 2c). E•INT was constructed from the X-ray structure of HIV-1 PR complexed with the highly peptidic MVT-101 inhibitor[34,36] (4HVP entry in the PDB data bank[44]), a compound that exhibits the sequence N-acetyl-Thr-Ile-Nle-Ψ[CH_2NH]-Nle-Gln-Arg-amide (Nle = norleucine). The Asp dyad was assumed to be monoprotonated according to the commonly accepted mechanism of HIV-1 PR.[36,39,41,42,45] The protein was immersed in a 90 × 71 × 74 Å^3 water box, and the entire system was neutralized by adding six chloride counterions. The whole system was composed of about 38 000 atoms.

2.2. Equilibration of E•INT. *2.2.1. Classical MD Simulations.* The complex was first equilibrated at the classical level using the AMBER9 suite of programs.[46] The parameters for the solute, apart from the amide hydrate (−C(OH)$_2$−NH−) moiety of the gem-diol intermediate, were taken from the AMBER 03 force field,[47] and the TIP3P model was used to describe water molecules.[48] Bonded and van der Waals parameters of the amide hydrate were extracted from the generalized AMBER force field (GAFF).[49] The charges of the amide hydrate were obtained using a standard RESP procedure.[50] The electrostatic potential was computed at the HF/6-31G(d) level with the Gaussian 03 package,[51] from a model compound including the hydrated Met−Met sequence capped with acetyl and N-methyl groups, i.e. Ace−Met−[C(OH)$_2$−NH]−Met−Nme. Note that these additional parameters are used for a small part only of the entire system, which is then described within the QM part during further equilibration at the QM/MM level (see next section).

Long-range electrostatic interactions were computed using the Ewald particle mesh method.[52,53] A cutoff of 10 Å was applied for the van der Waals interactions and the real part of the electrostatic interactions. A time step of 1.5 fs was used, and all bonds containing hydrogen were constrained using the SHAKE algorithm. Constant temperature was achieved using Langevin dynamics[54] with a collision frequency of 5 ps^{-1}, while the pressure was maintained using a Berendsen's barostat[55] with a relaxation time of 1.0 ps. The system was first heated to 150 K over 15 ps and then to 300 K over a further 15 ps. Then, an equilibration of 1 ns at 1 atm and 300 K was carried out.

2.2.2. QM/MM MD Simulations. Starting from the equilibrated E•INT structure obtained at the classical level, we switched to a hybrid quantum mechanics/molecular mechanics (QM/MM)[28] description for the system. We used the

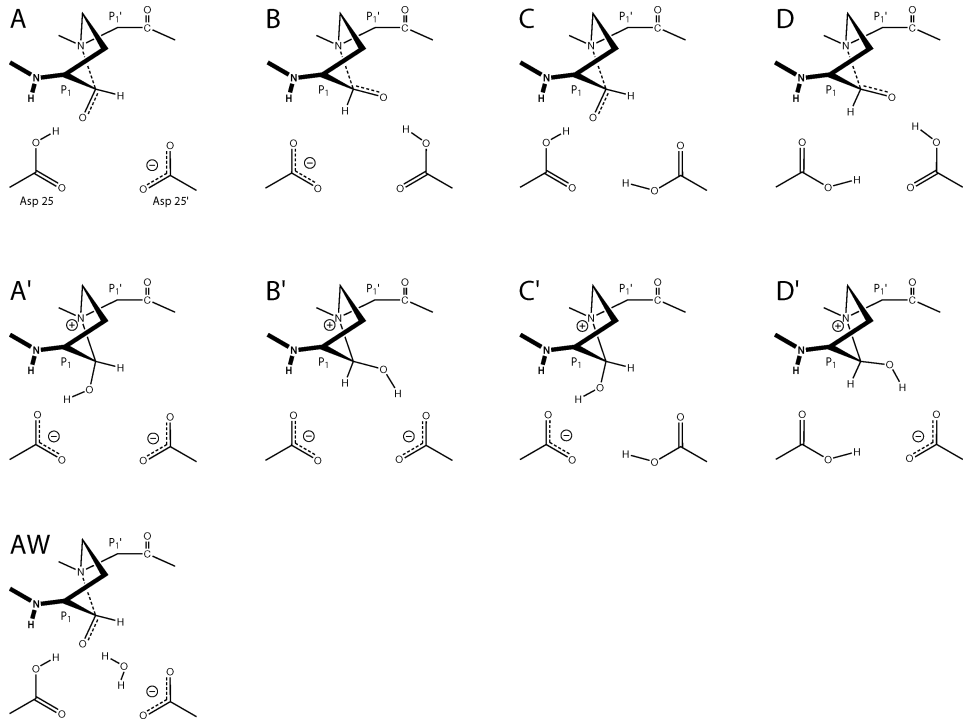

Figure 3. E•AAP isomers and protonation states considered in this study.

approach developed by Rothlisberger and co-workers.[56−58] The QM region encompassed the Asp25(25′) side chains and the amide hydrate moiety and was described at the DFT/BLYP[59,60] level of theory. Dangling bonds were saturated with hydrogen atoms. The Kohn−Sham orbitals were expanded in plane waves with a cutoff of 70 Ry and a quantum cell of 17.2 × 14.8 × 14.8 Å^3. A fictitious electron mass of 600 au and a time step of 5 au (≈ 0.12 fs) were used.

The E•INT system was first minimized using a simulated annealing-like procedure: starting from a temperature of 50 K, atomic velocities were rescaled at each time step by a factor of 0.99. Then, the system was heated up to 300 K over 15 ps. Subsequently, 12 ps of NVT simulation were performed, using a Nosé−Hoover chain thermostat[61−63] of 900 cm^{-1} frequency.

2.3. Transformation of E•INT into E•AAP. A structure obtained after 10.3 ps of simulation was chosen to perform the E•INT → E•AAP transformation. The hydrated substrate was modified at the Met−Met junction to incorporate the N···CO core and the aliphatic bridge (Figure 2b). The starting value of the characteristic C−N distance of the N···CO moiety was chosen to be 1.7 Å, which is a typical value for a N···CO bond in a polar-protic medium.[33] At this stage, we should stress that the only groups that differ from the initial crystallographic structure are the N···CO core and the aliphatic bridge. Once the peptide backbone of the AAP is accommodated in the active site, there are few possibilities left for the positioning of the cycle made of the aliphatic bridge and the N···CO group. The main uncertainty lies in the configuration of the carbon atom of the N···CO moiety. Thus we decided to study both possible configurations (Figure 3A,B).

Once the starting position of heavy atoms was chosen, we had to address the question of the active site protonation state within the E•AAP complex. Indeed, HIV-1 PR exhibits a wide range of protonation patterns according to the presence and the nature of the ligand.[39,45,64−71] The prediction of such a pattern can be done, for instance, by fitting kinetic data recorded at different pH to rate equations,[45,64] by computational pK_a estimation from an experimental structure,[65,66] by NMR titration,[67,68] by constructing computational models that aim at reproducing experimental data such as crystallographic structures[70,71] or NMR chemical shifts,[69] or by combining X-ray and neutron crystallography.[72]

The *a priori* determination of the E•AAP active-site protonation pattern is challenging. We decided to apply a systematic strategy, in which a series of protonation states for each configuration of the N···CO carbon atom was considered. When bound to neutral ligands, the aspartyl dyad of HIV-1 PR is usually monoprotonated[39,45,71,73] or diprotonated,[67] while positively charged ligands may yield an unprotonated dyad.[45,65]

Following this, we generated a series of nine isomers in different protonation states that are depicted in Figure 3.

First, we considered complexes A,B (monoprotonated dyad with neutral AAP) and C,D (diprotonated dyad with neutral AAP). In addition, the N···CO interaction can also be described by the limiting N$^+$−C−O$^-$ form. The negatively charged oxygen atom can be seen as an alcoholate and can thus be very basic. We have thus considered the possible proton transfer from the neighboring carboxyl group to the N···CO core leading to a positively charged AAP containing a N$^+$−CO−H moiety. A′,B′ (unprotonated dyad with positively charged AAP) and C′,D′ (monoprotonated dyad with positively charged AAP) were obtained from A,B and C,D, respectively, by shifting the closest proton of the Asp dyad to the N···CO oxygen atom.

To our knowledge, the catalytic water molecule that is tightly H-bonded to the aspartyl dyad in the HIV-1 PR-substrate complex (Figure 2c) is systematically displaced by any active site inhibitor bound to the enzyme. Indeed, it has only been observed in crystallographic structures of the free enzyme,[74,75] but never in any X-ray or NMR structure of the bound enzyme. However, we found it interesting to check if an AAP can displace this water molecule. Thus, we considered a last complex, denoted by AW, in which a water molecule is added close to the aspartyl dyad.

2.4. QM/MM Modeling of E•AAP Isomers in Different Protonation States. Once the E•INT → E•AAP transformation was performed, each E•AAP structure underwent a mild annealing-like protocol allowing a slow relaxation and minimization of the newly introduced aliphatic bridge−N···CO moiety and the surrounding protein medium. This enabled us to scrutinize (i) the stability of the N···CO bond within the protein and (ii) the interactions between the AAP and the protein.

We used the same level of calculation as the one we used to equilibrate E•INT. The QM region included the Asp25(25′) side chains, the N···CO moiety, and the aliphatic bridge. We stress that the ability of density functional theory to describe the N···CO interaction was demonstrated previously.[33] The quantum cell size was adapted to that of the QM region, leading to a 16.9 × 14.3 × 16.9 Å^3 box.

Each E•AAP complex underwent a first minimization, using the same simulated annealing-like procedure that we used previously to optimize the geometry of the E•INT complex, i.e., using a starting temperature of 50 K and a scaling factor of 0.99. These calculations were stopped as soon as the temperature reached a value below 3 K. Then, the system was let free to relax during 8 ps of NVE QM/MM molecular dynamics. During this run, each complex heated up to about 40 K due to remaining bad contacts. Finally, the minimization of the system was achieved using a second annealing with a scaling factor of 0.999.

To check the validity of this relaxation/optimization protocol, we performed further calculations using constraints. These calculations are described in the Supporting Information.

2.5. QM/MM Modeling of AAP in Water. The simulations in water were started from the same starting structure of the AAP as the one used in complex A. The inhibitor was immersed in a 49 × 49 × 49 Å^3 water box equilibrated at room temperature at the classical level. All of the atoms of the AAP were fixed during the first stages of the simulation. For the QM/MM runs, we used the same description as the one for the E•AAPs. The quantum cell size was adapted to that of the QM region, leading to a 11.0 × 11.3 × 10.4 Å^3 box.

The water box was further equilibrated using the following protocol: A first annealing was performed using a starting temperature of 50 K and a velocity scaling factor of 0.99. Then, the solvent underwent 4.7 ps of MD simulation at 300 K using the Berendsen weak coupling algorithm.[55] Finally, the target temperature was decreased linearly from 300 to 1 K in 3 ps.

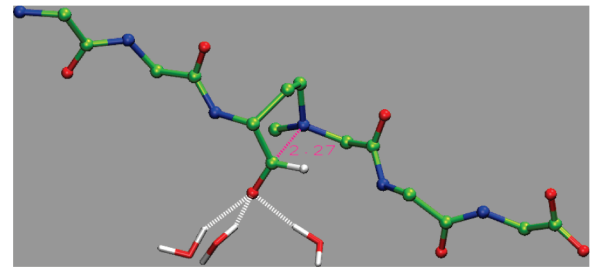

Figure 4. Optimized geometries of the AAP in water at the QM/MM level of theory. Only the inhibitor backbone and water molecules hydrogen bonded to the oxygen atom of the N···CO core are represented. The N···CO interaction is depicted in magenta.

At this stage, the constraints on the inhibitor were removed, and we minimized the QM and the MM part of the system consecutively. Then, the system underwent 4 ps of NVT simulation using a Nosé−Hoover chain thermostat.[61−63] Finally, a minimized geometry was obtained by performing an annealing with a velocity scaling factor of 0.999.

3. Results and Discussion

3.1. AAP in Water. We start the analysis of our results by describing the behavior of the N···CO bond embedded in an AAP in an aqueous medium. During our 4 ps of NVT simulation at 300 K, a weak N···CO interaction was maintained, with an average value of the C−N distance of 2.41 Å and a standard deviation of 0.18 Å. After minimization using our annealing-like protocol, this distance decreased to 2.27 Å. Figure 4 shows the corresponding optimized geometry. The nitrogen lone pair of the N···CO core is directed toward the aldehyde, which has lost its coplanarity. Three water molecules are hydrogen bonded to the aldehyde, which stabilizes the N···CO bond.

The fact that the N···CO bond is maintained over the course of the simulation shows that our computational approach is able to reproduce the closed configuration reported by Hasserodt et al.[19] On the basis of NMR measurements in methanol, they estimated that 70% of the AAPs exhibit a N···CO bond. We expect that much longer simulations would provide opening and closing events.

Nevertheless, the average C−N distance we observe is longer than the typical value of 1.8 Å of a N···CO bond in a polar-protic medium.[33] This is in agreement with the computational study of Pilmé et al., who have shown that water molecules H-bonded to the N···CO core stabilize the N^+−C−O^- form by accepting part of its electronic density.[33] Even though the charge transfer is small (ca. 0.06 e/molecule), it was shown to be sufficient to stabilize short CN distances. In our simulations, the interaction between the N···CO core and the surrounding water molecules is described through the QM/MM interface, which does not account for charge transfer effects, hence leading to a longer C−N distance. Note, however, that this problem does not hold for our simulations in HIV-1 PR (next sections), because the polar protein group close to the N···CO core was included in the QM part.

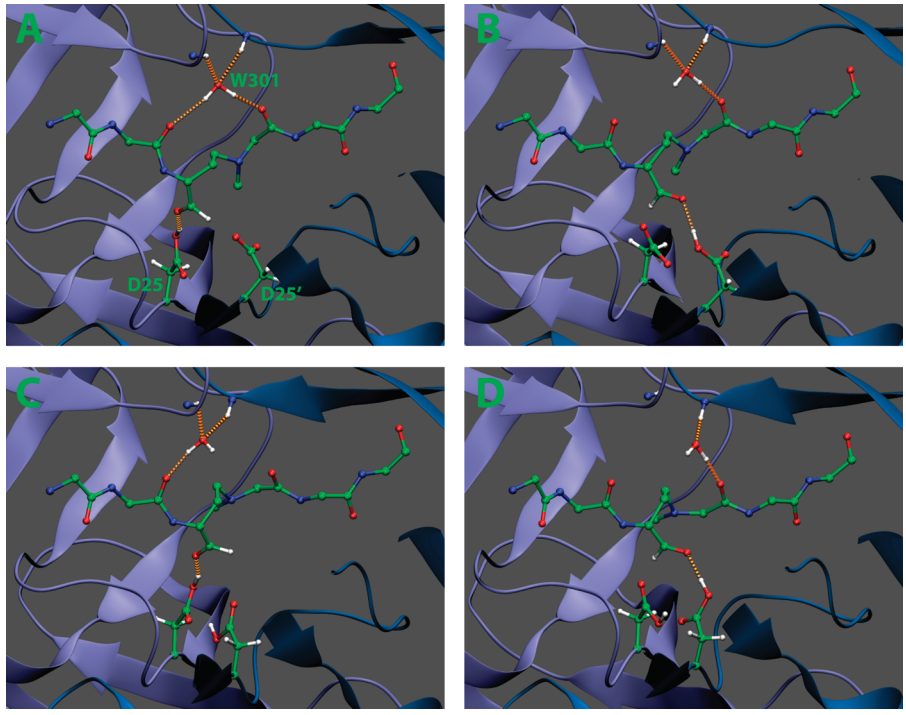

Figure 5. Optimized geometries of complexes A−D at the QM/MM level of theory. Only polar hydrogens belonging to the H-bond networks around W301, the N···CO core, and the aspartyl dyad are represented.

3.2. Protonation State of the N···CO Oxygen Atom in the Protein. The first question we addressed concerning the behavior of AAPs within HIV-1 PR was whether the protein is able to provide a stabilizing medium for a protonated, positively charged AAP. Indeed, due to the enhanced ionic character of the C−O bond within the N···CO core, the basicity of the oxygen is increased, and thus, a sufficiently acidic medium could stabilize a covalent N^{+}−CO−H moiety.

In the early stages of the minimization of isomers A′−D′, we observed that the proton linked to the N···CO oxygen was systematically shifted to the closest aspartate, leading to isomers A−D, respectively. Thus, despite the difficulty of providing an a priori accurate estimation of the protonation pattern in the active site of our system, our calculations consistently converge to an AAP N···CO core that is unprotonated within HIV-1 PR. Therefore, in the following, only isomers A−D and AW will be considered.

3.3. N···CO Bond Stability in the Active Site and Interaction with the Asp Dyad. Optimized geometries of complexes A−D are depicted in Figure 5. Selected structural parameters are reported in Table 1. For each complex, the characteristic C−N distance of the N···CO moiety exhibits a drastic lengthening from the starting value of 1.7 Å. Note that, since this opening event was already observed during geometry optimization, we did not attempt to run molecular dynamics simulations at room temperature, as we did for the modeling of AAPs in water. Instead, we applied a mild relaxation/minimization protocol in order to assess the effect of the enzymatic media on the geometry of AAPs.

Monoprotonated complexes A and B are stabilized in a fully opened conformation, with $d_{CN} = 3.75$ and 3.43 Å in A and B, respectively. This distance is larger than the characteristic value of even a weak N···CO interaction in which $d_{CN} \approx 2.8$ Å.[33] In both structures, the N···CO nitrogen lone pair is no longer directed toward the planar aldehyde group, indicating that the N···CO interaction is completely disrupted. Furthermore, the aspartyl dyad coplanarity is lost according to the values of the dihedral angle between each Asp oxygen, i.e., $\Omega = 94.2$ and 69.4° for A and B, respectively. This structural feature plays a crucial role in the binding of both substrate and inhibitors.[4,76,77] The highly distorted conformation of the aspartyl dyad is a clear indicator of an unfavorable interaction between the N···CO core, Asp25 and Asp25′. Despite the hydrogen bond between the proton of Asp25(25′) and the carbonyl oxygen of the AAP in isomer A(B) (see Table 1), the AAP does not provide sufficient shielding to stabilize the strong electrostatic Asp−Asp repulsion.[70]

Table 1. Main Geometrical Parameters Resulting from the Minimization of Complexes A−D[a]

	A	B	C	D
d_{CN}[b]	3.75	3.43	3.01	2.51
NCO···H$\delta_{Asp25(25')}$[c]	1.66	1.76	1.60	1.61
NH_{Ile50}···O_{W301}[d]	2.20	2.39	2.34	3.42
$NH_{Ile50'}$···O_{W301}[d]	2.26	2.01	2.08	1.87
CO_{P2}···H_{W301}[d]	2.30	3.67	1.77	4.28
$CO_{P1'}$···H_{W301}[d]	1.75	1.67	3.83	1.64
Ω[e]	94.25	69.44	37.77	−43.12
Φ[f]	−125.77	−84.81	−74.34	−51.06

[a] Distances are given in Å and angles in degrees. [b] Distance between the tertiary amine nitrogen and the aldehyde. [c] Hydrogen bond between the N···CO oxygen and the H_δ of the aspartyl dyad. Residue 25 or 25′ is considered, depending on the protonation pattern of the aspartyl dyad. [d] Hydrogen bond network around the structural water molecule W301. [e] Dihedral angle between each Asp oxygen of the aspartyl dyad. [f] Dihedral angle of the aliphatic bridge.

The AW complex (results not shown) follows a similar route, leading to a drastic lengthening of the C−N distance and the loss of the aspartyl dyad coplanarity. Moreover, the opening of the N···CO core is accompanied by the departure of the catalytic water molecule out of the aspartyl dyad, yielding a structure close to complex A. In fact, we observe that this water molecule is stabilized by a hydrogen bond with the Gly27 carbonyl group. Despite the short time scale that is accessible at the QM/MM level, we expect that this is a transient state, prior to a move of the catalytic water molecule to the bulk. We have already observed this behavior in a classical simulation of a HIV-1 PR-substrate complex (not presented here), which is consistent with observations reported by others.[40]

Diprotonated complex D exhibits the smallest C−N distance (d_{CN} = 2.51 Å), which corresponds to a weak N···CO interaction.[33] The nitrogen lone pair is still directed toward the carbonyl group which is less planar and more tightly H-bound to Asp25′ than in the monoprotonated complexes, according to the NCO···H$\delta_{Asp25'}$ distance. The Asp dyad remains almost coplanar, suggesting that the complex is much more stable than the monoprotonated ones. This is in agreement with the fact that the shielding introduced by the additional proton in diprotonated states makes the aspartyl dyad more amenable to accepting the accumulated negative charge of the N···CO oxygen.

Complex C represents an intermediate situation between complexes D and A,B. As in D, it is characterized by a coplanar aspartyl dyad and a tight hydrogen bond between the oxygen of the N···CO core and Asp25. However, similarly to A and B, the C−N distance equals 3.01 Å, which corresponds at best to a shallow N···CO bond.

Our systematic approach reflects the geometric behavior of the N···CO core within the enzyme, over a set of different conditions related to the protonation state and the starting configuration of the N···CO carbon atom. As we will show in the next section, our model enables one to establish a correlation between the disruption of the N···CO bond and other interactions that play a key role in the affinity between the AAP and HIV-1 PR.

3.4. Origin of the N···CO Opening. A detailed analysis of the hydrogen bond network inside the HIV-1 PR active site sheds some light on the origin of the instability of the N···CO bond within the enzyme. In HIV-1 PR−substrate and in most HIV-1 PR−inhibitor complexes,[78] a tetrahedrally coordinated structural water molecule, commonly labeled W301,[1,79,80] bridges Ile50(50′) NH groups belonging to the upper part of the active site cleft (the so-called *flaps*, Figure 1) and P_2 and P_1' CO groups of the substrate/inhibitor. Hence, this hydrogen bond network plays a crucial role in the correct positioning of both substrate and peptidomimetic inhibitors in the active site. Inhibitors that do not exhibit these interactions are those that have been designed to displace W301, such as cyclic urea derivatives[26] or the FDA-approved drug Tipranavir.[27]

Figure 6a depicts the starting geometry (just after the E•INT→E•AAP transformation) of W301 and its surrounding atoms within complex A. Note that the position of heavy atoms is the same as that of complex C and AW and is very similar to that of complexes B and D, the only difference being the configuration of the N···CO carbon atom. The tetrahedral H-bond network around W301 is present, prior to any step of our minimization protocol. In the starting configuration of our complexes, the "macrocycle" composed of W301, P_2, and P_1' CO groups and the aliphatic bridge (represented with orange transparent tubes in Figure 6) is in a quite compact conformation, while the C−N distance of the N···CO moiety is 1.7 Å.

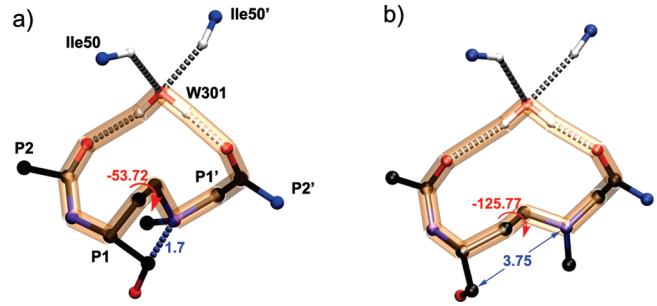

Figure 6. Competition between the N···CO bond formation and the conservation of the H-bond network around the structural water molecule W301. Starting (a) and final (b) geometries of W301 and its surrounding atoms within complex A. Side chains and hydrogen atoms not belonging to the H-bond network around W301 are not represented for the sake of simplicity. The "macrocycle" composed of W301, P_2, and P_1' CO groups and the aliphatic bridge is represented with orange transparent tubes. The H bonds around W301 are depicted with gray-dashed tubes, while the N···CO interaction is represented with a blue-dashed tube in the starting structure (a).

During the NVE molecular dynamics run of complex A, the H bonds around W301 are first partly disrupted, and as the C−N distance lengthens, the hydrogen bond network is progressively restored. Figure 6b represents the final (optimized) structure of complex A. The "macrocycle" is stabilized in an extended conformation, in which the aliphatic bridge has been pushed away from W301. This structural reorganization occurs together with a drastic increase of both the characteristic dihedral angle Φ of the aliphatic bridge (from −51 to −126°) and the C−N distance (from 1.7 to 3.75 Å). Hence, the disruption mechanism of the N···CO bond observed in complex A may be formulated as follows: The hydrogen bond network that W301 tends to form with two backbone carbonyl groups of the AAP tightens the "macrocycle", which in turn reduces the steric hindrance by extending the aliphatic bridge, thus lengthening the C−N distance of the N···CO core.

Complex B exhibits a behavior similar to that of complex A, sharing the same location of W301 and the evolution of the structure toward an extended "macrocycle". The major difference lies in the value of the dihedral angle of the aliphatic bridge (Table 1), which is lower in B, i.e., Φ = −84.8°. Thus, the aliphatic bridge remains closer to the center of the "macrocycle", and W301 cannot establish an optimal hydrogen bond with the P_2 carbonyl.

In order to analyze the link between the hydrogen bond network around W301 and the CN distance, we have

conducted a constrained optimization. Starting from the optimized geometry of complex B, we changed the hydrogen bond network around the W301 molecule from that in complex B to that in complex A. The CN bond was not frozen, and we found that it increased to reach a final length of 3.70 Å, close to the value observed in complex A.

The situation is rather different for diprotonated complexes. In the optimized complexes C and D, W301 is no longer tetrahedrally coordinated, as depicted in Figure 5C,D. The highest disruption occurs for complex D, which conserves only two hydrogen bonds. On the other hand, the aliphatic bridge remains in a conformation closer to that of the starting structure, as indicated by the Φ values: −74.3 and −51.1° for C and D, respectively. This is consistent with the C−N distance values discussed in the previous section. As previously noted, a diprotonated dyad is a better hydrogen bond donor than a monoprotonated one and is thus more favorable to the N···CO interaction, which in turn, is more competitive against the conservation of the H-bond network around W301.

The behavior observed for complexes A−D can be summarized stating that a N···CO bond and a proper H-bond network around W301 cannot be realized both at the same time. Clearly, the introduction of the N···CO core at the scissile peptide bond location induces a systematic competition between the N···CO bond formation and the interaction network involving the structural water molecule W301. Barillari et al.[81] estimated the binding free energy of W301 to a series of complexes between HIV-1 PR and peptidomimetic inhibitors using the double-decoupling free energy simulation method. They found that the binding free energy ranged from −7 to −10 kcal mol^{-1}. If one removes the entropy contribution, in which the upper bound has been estimated to be about 2 kcal mol^{-1},[82] one obtains a binding energy of −(9−12) kcal mol^{-1}. This is comparable to the energy of the N···CO bond, which has been estimated to be −11 kcal mol^{-1} at the CCSD(T) level.[33] These energetic considerations support the competition that we observed between the conservation of the hydrogen bond network around W301 and N···CO bond formation.

Since the N···CO moiety has been designed to interact strongly with the aspartyl dyad,[19] our simulations show that an AAP cannot provide stabilizing interactions with all the key parts of the HIV-1 PR binding site at the same time. The low inhibition power of AAPs might originate, at least partly, from this competition. Interestingly, our results suggest that further development of N···CO containing inhibitors should focus on nonpeptidic compounds that could displace W301. This in line with the hydrazino-urea compounds proposed recently by Hasserodt et al.[20,21] These derivatives contain both a N···CO bond and a hydrazino-urea group designed to interact directly with the flaps of HIV-1 PR, similar to cyclic urea derivatives[26] and the FDA-approved drug Tipranavir.[27]

Note that hydrazino−urea compounds synthesized by Hasserodt et al. bind only slightly stronger to HIV-1 PR than AAPs ($K_i \approx 29$ μM and 97 μM, respectively). However, the former contain only three groups aimed at filling the subpockets of the enzyme binding cleft, while cyclic urea derivatives usually have four.[26] Hence, we encourage the development of optimized N···CO-containing hydrazino−urea inhibitors that would contain proper groups aimed at interacting with the same binding subpockets as cyclic urea derivatives. Such a design could be assisted by a computational study based on the same approach we developed in the present work.

4. Conclusions

We have proposed here a computational procedure to tackle the difficult theoretical description of HIV-1 PR inhibitors based on the unusual N···CO bond. This procedure consists of an explicitly solvated model of the ligand−enzyme complex (E•AAP) described at the atomistic level with a QM/MM approach. The N···CO core and part of the enzyme active site are described using an accurate QM level, while the rest of the protein and the solvent are described using the classical AMBER force field.

In this work, we have applied this model to investigate the origin of the low inhibiting power of the recently proposed amino-aldehyde peptide (AAP) compounds against HIV-1 PR. Our calculations provide detailed information on the feasibility of the N···CO bond formation within the enzymatic environment along with crucial interactions that govern the stability of the complex.

Considering all the possible protonation patterns of the active site aspartyl dyad, we have shown that N···CO bond formation/dissociation takes place in a competitive mechanism, in which the structural water molecule W301 tends to establish a hydrogen bond network that indirectly penalizes the shortening of the distance between the nitrogen atom and the CO group of the N···CO core. We conclude that the reported poor inhibition power of AAPs[19] originates, at least partly, from this competition.

Despite this, a N···CO···H$\delta_{Asp25(25')}$ hydrogen bond was observed for each protonation state. In the case of complex D, this H bond is tighter, and a weak N···CO interaction is formed at the same time. This means that, under appropriate conditions, a N···CO core could interact strongly with the aspartyl dyad of HIV-1 PR. Hence, the design of N···CO-containing candidates that could displace the water molecule W301 would be an interesting alternative to AAPs. This supports the idea that a hydrazino−urea core[20,21] is an interesting template for the design of potent anti-AIDS drugs. In particular, it would be interesting to extend the recent work of Hasserodt et al. to hydrazino−urea derivatives containing peripheral groups aimed at filling the HIV-1 PR subpockets P_2, P_1, P_1', P_2' properly, similar to cyclic urea derivatives. Such a design could be done *in silico*, using the approach we have developed in the present study.

Acknowledgment. We thank the "Centre Informatique National de l'Enseignement Supérieur" and the "Institut du développement et des ressources en informatique Scientifique" for computational support and resources. We also thank Dr. M. Waibel and Pr. J. Hasserodt for useful

discussions. The financial support from the "Cluster de recherche Chimie de la Région Rhone-Alpes" is duly acknowledged.

Abbreviations

HIV-1, Human Immunodeficiency Virus Type 1; AIDS, Acquired ImmunoDeficiency Syndrome; PR, Protease; E, catalytically active dimeric form of HIV-1 protease; INT, Thr−Ile−Met−Met−Gln−Arg peptide substrate in its hydrated form; QM/MM, Quantum Mechanics/Molecular Mechanics; FDA, Food and Drug Administration; AAP, Amino-Aldehyde Peptide; CPMD, Car−Parrinello Molecular Dynamics; DFT, Density Functional Theory.

Supporting Information Available: The results of the additional simulations with various constrained distances (d_{CN}, $NH_{Ile50}\cdots O_{W301}$, $NH_{Ile50'}\cdots O_{W301}$, $CO_{P2}\cdots H_{W301}$, $CO_{P1'}\cdots H_{W301}$) are described. This material is available free of charge via the Internet at http://pubs.acs.org.

References

(1) Wlodawer, A.; Vondrasek, J. *Annu. Rev. Biophys. Biomol. Struct.* **1998**, *27*, 249–284.

(2) Wlodawer, A.; Erickson, J. W. *Annu. Rev. Biochem.* **1993**, *62*, 543–585.

(3) Debouck, C.; Gorniak, J. G.; Strickler, J. E.; Meek, T. D.; Metcalf, B. W.; Rosenberg, M. *Proc. Natl. Acad. Sci. U.S.A.* **1987**, *84*, 8903–8906.

(4) Fitzgerald, P. M. D.; Springer, J. P. *Annu. Rev. Biophys. Biophys. Chem.* **1991**, *20*, 299–320.

(5) Poorman, R.; Tomasselli, A.; Heinrikson, R.; Kezdy, F. *J. Biol. Chem.* **1991**, *266*, 14554–14561.

(6) Kohl, N. E.; Emini, E. A.; Schleif, W. A.; Davis, L. J.; Heimbach, J. C.; Dixon, R. A. F.; Scolnick, E. M.; Sigal, I. S. *Proc. Natl. Acad. Sci. U.S.A.* **1988**, *85*, 4686–4690.

(7) Seelmeier, S.; Schmidt, H.; Turk, V.; von der Helm, K. *Proc. Natl. Acad. Sci. U.S.A.* **1988**, *85*, 6612–6616.

(8) McQuade, T. J.; Tomasselli, A. G.; Liu, L.; Karacostas, V.; Moss, B.; Sawyer, T. K.; Heinrikson, R. L.; Tarpley, W. G. *Science* **1990**, *247*, 454–456.

(9) Richman, D. D. *Nature* **2001**, *410*, 995–1001.

(10) Hammer, S. M.; Squires, K. E.; Hughes, M. D.; Grimes, J. M.; Demeter, L. M.; Currier, J. S.; Eron, J. J.; Feinberg, J. E.; Balfour, H. H.; Deyton, L. R.; Chodakewitz, J. A.; Fischl, M. A.; Phair, J. P.; Pedneault, L.; Nguyen, B.-Y.; Cook, J. C. *N. Engl. J. Med.* **1997**, *337*, 725–733.

(11) Gulick, R. M.; Mellors, J. W.; Havlir, D.; Eron, J. J.; Gonzalez, C.; McMahon, D.; Richman, D. D.; Valentine, F. T.; Jonas, L.; Meibohm, A.; Emini, E. A.; Chodakewitz, J. A.; Deutsch, P.; Holder, D.; Schleif, W. A.; Condra, J. H. *N. Engl. J. Med.* **1997**, *337*, 734–739.

(12) Condra, J. H.; Schleif, W. A.; Blahy, O. M.; Gabryelski, L. J.; Graham, D. J.; Quintero, J.; Rhodes, A.; Robbins, H. L.; Roth, E.; Shivaprakash, M.; Titus, D.; Yang, T.; Tepplert, H.; Squires, K. E.; Deutsch, P. J.; Emini, E. A. *Nature* **1995**, *374*, 569–571.

(13) Martinez-Cajas, J. L.; Wainberg, M. A. *Antiviral Res.* **2007**, *76*, 203–221.

(14) Luque, I.; Todd, M. J.; Gómez, J.; Semo, N.; Freire, E. *Biochemistry* **1998**, *37*, 5791–5797.

(15) Velázquez-Campoy, A.; Kiso, Y.; Freire, E. *Arch. Biochem. Biophys.* **2001**, *390*, 169–175.

(16) Velázquez-Campoy, A.; Luque, I.; Freire, E. *Thermochim. Acta* **2001**, *380*, 217–227.

(17) Vega, S.; Kang, L.-W.; Velázquez-Campoy, A.; Kiso, Y.; Amzel, M.; Freire, E. *Proteins: Struct., Funct., Bioinf.* **2004**, *55*, 594–602.

(18) Leung, D.; Abbenante, G.; Fairlie, D. P. *J. Med. Chem.* **2000**, *43*, 305–341.

(19) Gautier, A.; Pitrat, D.; Hasserodt, J. *Bioorg. Med. Chem.* **2006**, *14*, 3835–3847. Kinetics and inhibition measurements are given in their Supplementary Data.

(20) Waibel, M.; Hasserodt, J. *J. Org. Chem.* **2008**, *73*, 6119–6126.

(21) Waibel, M.; Pitrat, D.; Hasserodt, J. *Bioorg. Med. Chem.* **2009**, *17*, 3671–3679.

(22) Shuman, C. F.; Hämäläinen, M. D.; Danielson, U. H. *J. Mol. Recognit.* **2004**, *17*, 106–119.

(23) Velázquez-Campoy, H. O. A.; Xie, D.; Freire, E. *Protein Sci.* **2002**, *11*, 1908–1916.

(24) Markgren, P.-O.; Schaal, W.; Hämäläinen, M.; Karlén, A.; Hallberg, A.; Samuelsson, B.; Danielson, U. H. *J. Med. Chem.* **2002**, *45*, 5430–5439.

(25) Velázquez-Campoy, A.; Freire, E. *J. Cell. Biochem.* **2001**, *37*, 82–88.

(26) Lam, P. Y. S.; Ru, Y.; Jadhav, P. K.; Aldrich, P. E.; DeLucca, G. V.; Eyermann, C. J.; Chang, C.-H.; Emmett, G.; Holler, E. R.; Daneker, W. F.; Li, L.; Confalone, P. N.; McHugh, R. J.; Han, Q.; Li, R.; Markwalder, J. A.; Seitz, S. P.; Sharpe, T. R.; Bacheler, L. T.; Rayner, M. M.; Klabe, R. M.; Shum, L.; Winslow, D. L.; Kornhauser, D. M.; Jackson, D. A.; Erickson-Viitanen, S.; Hodge, C. N. *J. Med. Chem.* **1996**, *39*, 3514–3525.

(27) Doyon, L.; Tremblay, S.; Bourgon, L.; Wardrop, E.; Cordingley, M. G. *Antiviral Res.* **2005**, *68*, 27–35.

(28) Warshel, A.; Levitt, M. *J. Mol. Biol.* **1976**, *103*, 227–249.

(29) Spanka, G.; Boese, R.; Rademacher, P. *J. Org. Chem.* **1987**, *52*, 3362–3367.

(30) Griffith, R.; Bremner, J. B.; Titmuss, S. J. *J. Comput. Chem.* **1997**, *18*, 1211–1221.

(31) Leonard, N. J.; Oki, M. *J. Am. Chem. Soc.* **1954**, *76*, 3463–3465.

(32) Kirby, A. J.; Komarov, I. V.; Bilenko, V. A.; Davies, J. E.; Rawson, J. M. *Chem. Commun.* **2002**, 2106.

(33) Pilmé, J.; Berthoumieux, H.; Robert, V.; Fleurat-Lessard, P. *Chem.—Eur. J.* **2007**, *13*, 5388–5393.

(34) Miller, M.; Schneiderand, J.; Sathyanarayana, B.; Tothand, M.; Marshalland, G.; Clawsonand, L.; Selkand, L.; Kent, S.; Wlodawer, A. *Science* **1989**, *246*, 1149–1152.

(35) Prabu-Jeyabalan, M.; Nalivaika, E.; Schiffer, C. A. *Structure* **2002**, *10*, 369–381.

(36) Hyland, L. J.; Tomaszek, T. A., Jr.; Roberts, G. D.; Carr, S. A.; Magaard, V. W.; Bryan, H. L.; Michael, S. A. F.; Moore, L.; Minnich, M. D.; Culp, J. S.; DesJarlais, R. L.; Meek, T. D. *Biochemistry* **1991**, *30*, 8441–8453.

(37) Kovalevsky, A. Y.; Chumanevich, A. A.; Liu, F.; Louis, J. M.; Weber, I. T. *Biochemistry* **2007**, *46*, 14854–14864.

(38) Kumar, M.; Prashar, V.; Mahale, S.; Hosur, M. V. *Biochem. J.* **2005**, *389*, 365–371.

(39) Piana, S.; Bucher, D.; Carloni, P.; Rothlisberger, U. *J. Phys. Chem. B* **2004**, *108*, 11139–11149.

(40) Carnevale, V.; Raugei, S.; Piana, S.; Carloni, P. *Comput. Phys. Commun.* **2008**, *179*, 120–123.

(41) Trylska, J.; Grochowski, P.; McCammon, J. A. *Protein Sci.* **2004**, *13*, 513–528.

(42) Bjelic, S.; Aqvist, J. *Biochemistry* **2006**, *45*, 7709–7723.

(43) Ratner, L.; Haseltine, W.; Patarca, R.; Livak, K. J.; Starcich, B.; Josephs, S. F.; Doran, E. R.; Rafalski, J. A.; Whitehorn, E. A.; Baumeister, K.; Ivanoff, L.; Petteway, S. R., Jr.; Pearson, M. L.; Lautenberger, J. A.; Papas, T. S.; Ghrayeb-parallel, J.; Changparallel, N. T.; Gallo, R. C.; Wong-Staal, F. *Nature* **1985**, *313*, 277–284.

(44) Berman, H. M.; Westbrook, J.; Feng, Z.; Gilliland, G.; Bhat, T. N.; Weissig, H.; Shindyalov, I. N.; Bourne, P. E. *Nucleic Acids Res.* **2000**, *28*, 235–242.

(45) Hyland, L. J.; Tomaszek, T. A., Jr.; Meek, T. D. *Biochemistry* **1991**, *30*, 8454–8463.

(46) Case, D.; Darden, T.; Cheatham, T., III; Simmerling, C.; Wang, J.; Duke, R.; Luo, R.; Merz, K.; Pearlman, D.; Crowley, M.; Walker, R.; Zhang, W.; Wang, B.; Hayik, S.; Roitberg, A.; Seabra, G.; Wong, K.; Paesani, F.; Wu, X.; Brozell, S.; Tsui, V.; Gohlke, H.; Yang, L.; Tan, C.; Mongan, J.; Hornak, V.; Cui, G.; Beroza, P.; Mathews, D.; Schafmeister, C.; Ross, W.; Kollman, P. *AMBER 9*; University of California: San Francisco, 2006.

(47) Duan, Y.; Wu, C.; Chowdhury, S.; Lee, M. C.; Xiong, G.; Zhang, W.; Yang, R.; Cieplak, P.; Luo, R.; Lee, T.; Caldwell, J.; Wang, J.; Kollman, P. *J. Comput. Chem.* **2003**, *24*, 1999–2012.

(48) Jorgensen, W. L.; Chandrasekhar, J.; Madura, J. D.; Impey, R. W.; Klein, M. L. *J. Chem. Phys.* **1983**, *79*, 926–935.

(49) Wang, J.; Wolf, R. M.; Caldwell, J. W.; Kollman, P. A.; Case, D. A. *J. Comput. Chem.* **2004**, *25*, 1157–1174.

(50) Bayly, C. I.; Cieplak, P.; Cornell, W.; Kollman, P. A. *J. Phys. Chem.* **1993**, *97*, 10269–10280.

(51) Frisch, M. J.; Trucks, G. W.; Schlegel, H. B.; Scuseria, G. E.; Robb, M. A.; Cheeseman, J. R.; Montgomery, J. A., Jr.; Vreven, T.; Kudin, K. N.; Burant, J. C.; Millam, J. M.; Iyengar, S. S.; Tomasi, J.; Barone, V.; Mennucci, B.; Cossi, M.; Scalmani, G.; Rega, N.; Petersson, G. A.; Nakatsuji, H.; Hada, M.; Ehara, M.; Toyota, K.; Fukuda, R.; Hasegawa, J.; Ishida, M.; Nakajima, T.; Honda, Y.; Kitao, O.; Nakai, H.; Klene, M.; Li, X.; Knox, J. E.; Hratchian, H. P.; Cross, J. B.; Bakken, V.; Adamo, C.; Jaramillo, J.; Gomperts, R.; Stratmann, R. E.; Yazyev, O.; Austin, A. J.; Cammi, R.; Pomelli, C.; Ochterski, J. W.; Ayala, P. Y.; Morokuma, K.; Voth, G. A.; Salvador, P.; Dannenberg, J. J.; Zakrzewski, V. G.; Dapprich, S.; Daniels, A. D.; Strain, M. C.; Farkas, O.; Malick, D. K.; Rabuck, A. D.; Raghavachari, K.; Foresman, J. B.; Ortiz, J. V.; Cui, Q.; Baboul, A. G.; Clifford, S.; Cioslowski, J.; Stefanov, B. B.; Liu, G.; Liashenko, A.; Piskorz, P.; Komaromi, I.; Martin, R. L.; Fox, D. J.; Keith, T.; Al-Laham, M. A.; Peng, C. Y.; Nanayakkara, A.; Challacombe, M.; Gill, P. M. W.; Johnson, B.; Chen, W.; Wong, M. W.; Gonzalez, C.; Pople, J. A. *Gaussian 03*, Revision 02; Gaussian, Inc.: Wallingford, CT, 2004.

(52) Darden, T.; York, D.; Pedersen, L. *J. Chem. Phys.* **1993**, *98*, 10089–10092.

(53) Essmann, U.; Perera, L.; Berkowitz, M. L.; Darden, T.; Lee, H.; Pedersen, L. G. *J. Chem. Phys.* **1995**, *103*, 8577–8593.

(54) Izaguirrei, J. A.; Catarello, D. P.; Wozniak, J. M.; Skeel, R. D. *J. Chem. Phys.* **2001**, *114*, 2090–2098.

(55) Berendsen, H. J. C.; Postma, J. P. M.; van Gunsteren, W. F.; DiNola, A.; Haak, J. R. *J. Chem. Phys.* **1984**, *81*, 3684–3690.

(56) Car, R.; Parrinello, M. *Phys. Rev. Lett.* **1985**, *55*, 2471–2474.

(57) Laio, A.; VandeVondele, J.; Rothlisberger, U. *J. Chem. Phys.* **2002**, *116*, 6941–6947.

(58) Laio, A.; Gervasio, F. L.; VandeVondele, J.; Sulpizi, M.; Rothlisberger, U. *J. Phys. Chem. B* **2004**, *108*, 7963–7968.

(59) Becke, A. D. *Phys. Rev. A* **1998**, *38*, 3098–3100.

(60) Lee, C.; Yang, W.; Parr, R. G. *Phys. Rev. B* **1988**, *37*, 785–789.

(61) Nosé, S. *J. Chem. Phys.* **1984**, *81*, 511–519.

(62) Hoover, W. G. *Phys. Rev. A* **1985**, *31*, 1695–1697.

(63) Martyna, G. J.; Klein, M. L.; Tuckerman, M. *J. Chem. Phys.* **1992**, *97*, 2635–2643.

(64) Ido, E.; ping Han, H.; Kezdy, F. J.; Tang, J. *J. Biol. Chem.* **1991**, *266*, 24359–24366.

(65) Czodrowski, P.; Sotriffer, C. A.; Klebe, G. *J. Chem. Inf. Model.* **2007**, *47*, 1590–1598.

(66) Trylska, J.; Antosiewicz, J.; Geller, M.; Hodge, C.; Klabe, R.; Head, M.; Gilson, M. *Protein Sci.* **1999**, *8*, 180–195.

(67) Yamazaki, T.; Nicholson, L. K.; Wingfield, D. A. T. P.; Stahl, S. J.; Kaufman, J. D.; Eyermann, C. J.; Hodge, C. N.; Lam, P. Y. S.; Ru, Y.; Jadhav, P. K.; Chang, C.-H.; Webers, P. C. *J. Am. Chem. Soc.* **1994**, *116*, 10791–10792.

(68) Wang, Y.-X.; Freedberg, D. I.; Yamazaki, T.; Wingfield, P. T.; Stahl, S. J.; Kaufman, J. D.; Kiso, Y.; Torchia, D. A. *Biochemistry* **1996**, *35*, 9945–9950.

(69) Piana, S.; Sebastiani, D.; Carloni, P.; Parrinello, M. *J. Am. Chem. Soc.* **2001**, *123*, 8730–8737.

(70) Piana, S.; Carloni, P. *Proteins* **2000**, *39*, 26–36.

(71) Harte, W. E., Jr.; Beveridge, D. L. *J. Am. Chem. Soc.* **1993**, *115*, 3883–3886.

(72) Adachi, M.; Ohhara, T.; Kurihara, K.; Tamada, T.; Honjo, E.; Okazaki, N.; Arai, S.; Shoyama, Y.; Kimura, K.; Matsumura, H.; Sugiyama, S.; Adachi, H.; Takano, K.; Mori, Y.; Hidaka, K.; Kimura, T.; Hayashi, Y.; Kiso, Y.; Kuroki, R. *Proc. Natl. Acad. Sci. U.S.A.* **2009**, *106*, 4641–4646.

(73) Tawa, G. J.; Topol, I. A.; Burt, S. K.; Erickson, J. W. *J. Am. Chem. Soc.* **1998**, *120*, 8856–8863.

(74) Pillai, B.; Kannan, K.; Hosur, M. V. *Proteins* **2001**, *43*, 57–64.

(75) Kumar, M.; Hosur, M. V. *Eur. J. Biochem.* **2003**, *270*, 1231–1239.

(76) Davies, D. R. *Annu. Rev. Biophys. Biophys. Chem.* **1990**, *19*, 189–215.

(77) Todd, M. J.; Semo, N.; Freire, E. *J. Mol. Biol.* **1998**, *283*, 475–488.

(78) Vondrasek, J.; Wlodawer, A. *Proteins* **2002**, *49*, 429–431.

(79) Swain, A. L.; Miller, M. M.; Green, J.; Rich, D. H.; Schneider, J.; Kent, S. B. H.; Wlodawer, A. *Proc. Natl. Acad. Sci. U.S.A.* **1990**, *87*, 8805–8809.

(80) Jaskolski, M.; Tomasselli, A. G.; Sawyer, T. K.; Staples, D. G.; Heinrikson, R. L.; Schneider, J.; Kent, S. B. H.; Wlodawer, A. *Biochemistry* **1991**, *30*, 1600–1609.

(81) Barillari, C.; Taylor, J.; Viner, R.; Essex, J. W. *J. Am. Chem. Soc.* **2007**, *129*, 2577–2587.

(82) Dunitz, J. D. *Science* **1994**, *264*, 670–671.

(83) Humphrey, W.; Dalke, A.; Schulten, K. *J. Mol. Graphics* **1996**, *14*, 33–38.

(84) Schechter, I.; Berger, A. *Biochem. Biophys. Res. Commun.* **1967**, *27*, 157–162.

CT9004728